"Shaking in 5 Seconds!"—Performance and User Appreciation Assessment of the Earthquake Network Smartphone-Based Public Earthquake Early Warning System

Rémy Bossu[1,2] , Francesco Finazzi[*3] , Robert Steed[1], Laure Fallou[1] , and István Bondár[4]

Abstract

Public earthquake early warning systems have the potential to reduce individual risk by warning people of approaching tremors, but their development has been hampered by costly infrastructure. Furthermore, both users' understanding of such a service and their reactions to actual warnings have been the topic of only a few surveys. The smartphone app of the Earthquake Network initiative utilizes users' smartphones as motion detectors and provides the first example of a purely smartphone-based earthquake early warning system, without the need for dedicated seismic station infrastructure and operating in multiple countries. We demonstrate that this system has issued early warnings in multiple countries, including for damaging shaking levels, and hence that this offers an alternative to conventional early warning systems in the foreseeable future. We also show that although warnings are understood and appreciated by users, notably to get psychologically prepared, only a fraction take protective actions such as "drop, cover, and hold."

Introduction

Earthquake early warning (EEW) systems aim to warn people or infrastructure of imminent shaking through the rapid detection of earthquakes. Public earthquake early warning (PEEW) systems specifically target people rather than infrastructure and strive to reduce an individual's risk by allowing them to take protective actions (such as "drop, cover, and hold") in the seconds or tens of seconds separating the warning from ground shaking at the user's location. They were deployed first in 1991 in Mexico City (Suárez *et al.*, 2009) and then in Japan in 2007 (Nakayachi *et al.*, 2019). Despite this desirable goal and the existence of a number of other implementations, such as ShakeAlert in the western United States (Given *et al.*, 2018; Kohler *et al.*, 2018), Taiwan (Hsiao *et al.*, 2009; Xu *et al.*, 2017) and some private initiatives in Mexico and Chile, so far PEEW systems have not been put into service more widely, even in regions of high-earthquake hazard, because they require dense, real time, and robust seismic and communication networks (Cremen and Galasso, 2020). Furthermore, PEEW evaluations have mainly focused on technical performance (e.g., rapidity, false alert rate and missed alert rate) with only a few studies carried out from users' perspectives that assess how the service is valued and whether users react or not after receiving a warning (Suárez *et al.*, 2009; Nakayachi *et al.*, 2019), or how they anticipate reacting for a future service (Becker *et al.*, 2020). This situation has led to a lack of actual assessment of PEEW in terms of individual risk reduction so that key parameters such as the public's tolerance to false and missed alerts remain unknown, making it difficult to develop informed and efficient warning strategies (Allen and Melgar, 2019; Cochran and Husker, 2019).

Smartphones, due to their internal accelerometers, communication capabilities, and their ubiquity were rapidly identified for their low-cost potential for EEW (Minson *et al.*, 2015; Kong *et al.*, 2016). The Earthquake Network (EQN) initiative (Finazzi, 2016; Finazzi and Fassò, 2017; Finazzi, 2020a) implemented the first smartphone-based PEEW system that both detects earthquakes in real time and also publishes the earthquake warnings that the network generates. The feasibility of building a monitoring network from participants' smartphones has been further demonstrated by Kong *et al.* (2020a,b), and the results of a six-month study were recently published on creating a seismic network using fixed dedicated smartphones

1. European-Mediterranean Seismological Centre, Arpajon, France, https://orcid.org/0000-0002-9927-9122 (RB); https://orcid.org/0000-0002-0245-6197 (LF); 2. CEA, DAM, DIF, F-91297 Arpajon, France; 3. Department of Management, Information and Production Engineering, University of Bergamo, Dalmine, Italy, https://orcid.org/0000-0002-1295-7657 (FF); 4. Institute for Geological and Geochemical Research, Research Centre for Astronomy and Earth Sciences, Eötvös Loránd Research Network (ELKH), Budapest, Hungary, https://orcid.org/0000-0002-4892-1074 (IB)

*Corresponding author: francesco.finazzi@unibg.it

© Seismological Society of America

in Costa Rica (Brooks *et al.*, 2021), but these systems did not issue their own early warnings. In addition, Google announced in April 2021 that it has started a project to use Android smartphones to detect earthquakes and publish PEEW (Voosen, 2021). Google's system was initially tested in New Zealand and Greece, and is gradually being expanded to more regions. It appears to operate similarly to EQN; however, at the current time, no details are available on its implementation, and there are no published analyses of its efficacy.

The smartphone app of the EQN initiative turns participants' smartphones into real-time seismic detectors by monitoring their internal accelerometers while their phones are charging. The resulting monitoring network is fully dynamic, with new users often joining after feeling earthquakes and users often slowly leaving during calm periods. Since its inception in 2012, EQN has grown its userbase with 8 million app downloads and 1.2 million active users in July 2021, but this work is the first evaluation of its ability to provide early warnings.

When an active (i.e., charging) smartphone senses an acceleration above a noise-dependent threshold, a smartphone trigger is sent to the EQN servers, and timestamped upon reception. No attempt is made to analyze waveforms from the phones' accelerometers; instead, a detection occurs when the number of triggers within 30 km of each other and within a 10 s time frame exceeds a dynamic acceleration amplitude threshold that is a function of the actual number of active smartphones and of the desired false alarm probability—a level currently set to one per year per country (Finazzi and Fassò, 2017). Hereafter, a trigger will describe the motion detection performed by a single smartphone, whereas detection will refer to the EQN system detecting an earthquake through a statistical analysis of the collected individual triggers. A geo-located alert is issued at detection time to all users within 300 km of the detection location. This location is the centroid of the triggered smartphones, and it is taken as a proxy for the epicentral location. The alert is a smartphone notification with an easily recognizable sound and an automatic display of the epicentral location proxy, as well as a countdown in seconds to the estimated *S*-wave arrival time at the user location (Fig. 1). Large earthquakes can cause several detections. To avoid multiple alerts for the same earthquake, only detections at least 300 km and 120 s apart are released. EQN does not estimate the magnitude or intensity of events, which may not be appropriate for critical infrastructure stakeholders such as train operators or nuclear power plants. Instead, EQN is designed to provide value for the general public by focusing exclusively on disseminating information and issuing early earthquake warnings to the population.

The objectives of this work are to (1) evaluate EQN's detection performance, (2) demonstrate that it is capable of providing PEEW in multiple countries, and (3) assess the potential of EQN's contribution to individual risk reduction by studying EQN users' reactions after an actual early warning. One of the purposes of this article is to ascertain whether the service is still appreciated without the presence of intensity predictions. Performance has been evaluated over a 26-month period (from 15 December 2017 to 31 January 2020) during which the EQN data processing methodology was not modified. In addition, reaction to and understanding of early warning by EQN users has been inferred from an online survey of local EQN users in the felt area of the 2019 **M** 8 Peru earthquake.

Results
EQN detection performance
EQN's detection performance in terms of latency, false detection rate, and missed earthquake detections has been evaluated using 550 detections from Chile, United States, and Italy. These are the three countries that had at least 10 detections and had national catalogs that possessed both good location accuracy and coverage of low-magnitude earthquakes, and additionally had accelerometric data available. Accurate locations are required to make proper estimates of the system's latency, and catalogs including low-magnitude earthquakes are essential for both network sensitivity and false detection rate estimates as smartphone detections are possible down at least to **M** 2 (Kong *et al.*, 2020a). Finally, accelerometric data were sought out from available scientific-grade stations close to each detection location for a final consistency check against waveform data.

EQN detections were first associated in time and space with hypocenters from national catalogs; then, among the potential candidates, an earthquake was considered as the source of the detection if the theoretical arrival time of the *P* wave at the detection location was between 90 s before and 10 s after the detection time. The 90 s lead time was primarily to allow the association of detections triggered by the *S* phase as well as location and velocity model uncertainties. This led to an initial association of 535 out of 550 detections. For this analysis, whenever an accelerometric station was available within 20 km of the detection location (410 out of 550 detections), the existence and time consistency of ground motion was visually checked. This inspection enabled association with earthquakes for four additional detections. One was associated to an **M** 3.8 earthquake at an unusually large distance of 350 km and two to small-magnitude earthquakes (**M** 1.4 and 1.5 located 2 and 8 km from the detection, respectively) located through additional investigation by the Seismological Centre of the University of Chile. The fourth was found to be a secondary detection 800 km from epicenter of the 1 March 2019 **M** 7.0 Peru earthquake. A number of detections cannot be associated to any known earthquake leading to a false detection rate of ~2%.

The 539 associated detections are consistent with previous detectability study of smartphone sensors (Kong *et al.*, 2019). With half related to earthquakes below **M** 4 (Fig. 2), there are
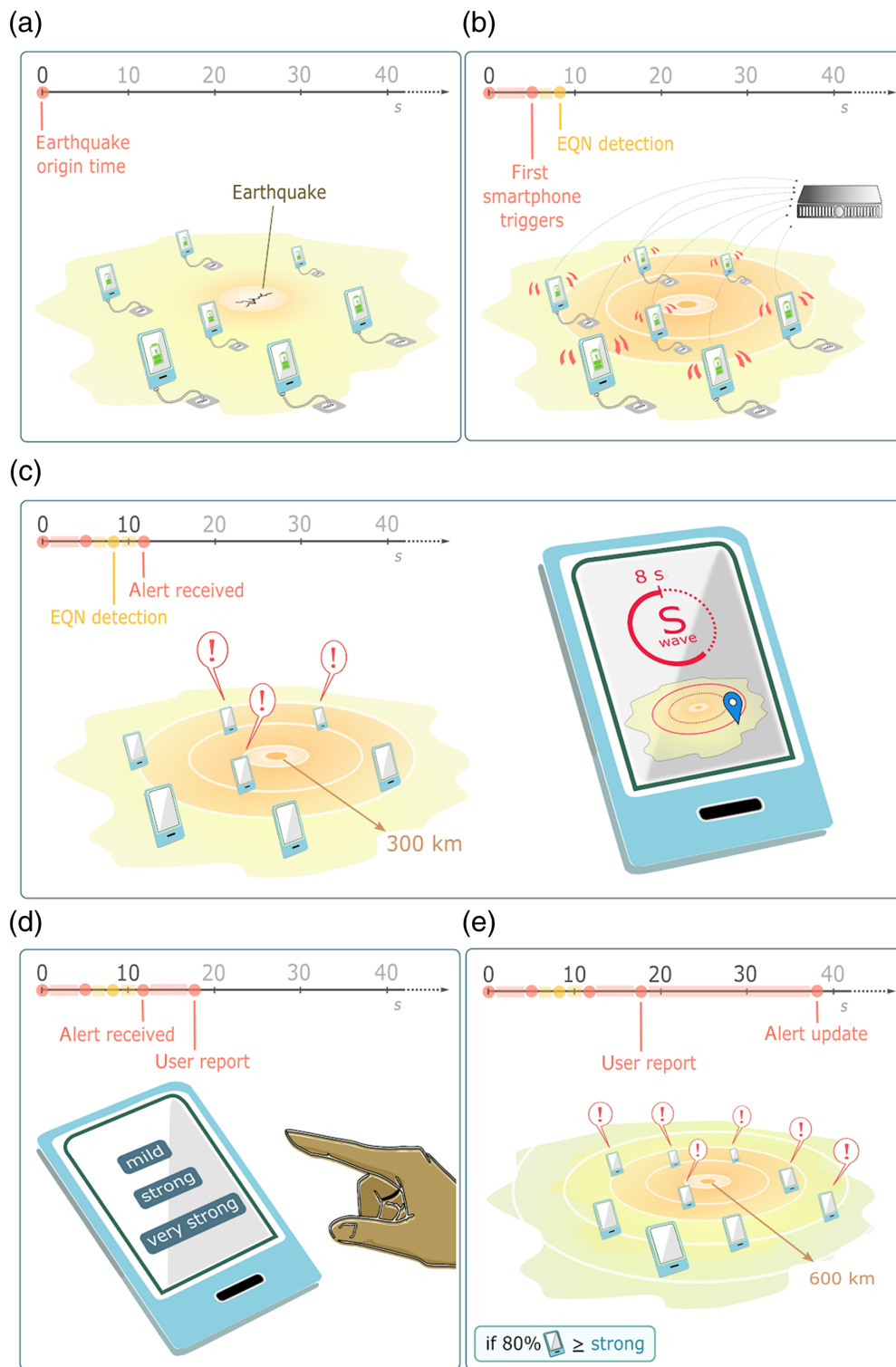
Figure 1. (a) The Earthquake Network (EQN) app turns a charging smartphone into a ground-motion detector. Earthquakes are detected through a cluster of smartphone triggers. (b) Once detected, an alert is issued to all users within a default distance of the detection, and (c) a countdown of the estimated S-wave arrival time is displayed at the user's location. (d) Users can qualitatively report the level of shaking if they choose to, with three levels (Finazzi, 2020b). This is intended to identify larger earthquakes, as EQN does not provide magnitude estimates. (e) If at least 10% of the users in the area of detection submit reports, and 80% of these reports are "strong" or "very strong," a second alert is issued (typically 30 s after the first one) to users in an enlarged region (600 km by default). Users can opt in or out of the two alerts and customize alerting distances. The color version of this figure is available only in the electronic edition.

many events that are unlikely to have generated strong shaking and therefore for which an early warning may not have been necessary. However, comparison with independent data (Fig. 2) indicates that nearly all of the EQN detections are likely to have also been felt, which make them relevant for rapid public information, even the few that were very low magnitude.

Assessment of EQN's rate of missed earthquakes is more complex than for traditional seismic monitoring networks, as the network geometry is governed by spatiotemporal variations in population distribution—higher in cities, lower in low-population areas—and it constantly changes with app installations and deletions, and the number of active smartphones. Hence, EQN detectability generally increases at night when more phones are charging. The rate of EQN earthquake detections was 3.1 times higher at night than during the day (Table 1). Despite this variability, in Italy where the number of app users (about 45,000) remained stable during the studied period the two largest earthquakes (**M** 5.1 and 4.9) were both detected, as well as four out of six earthquakes between **M** 4.5 and 4.9.

Latency of earthquake detections from a dynamic monitoring network

The shortest earthquake detection latencies, that is, the time difference between earthquake origin time and alert issuance, are achieved when the hypocenter is close to regions where the EQN app is popular. This
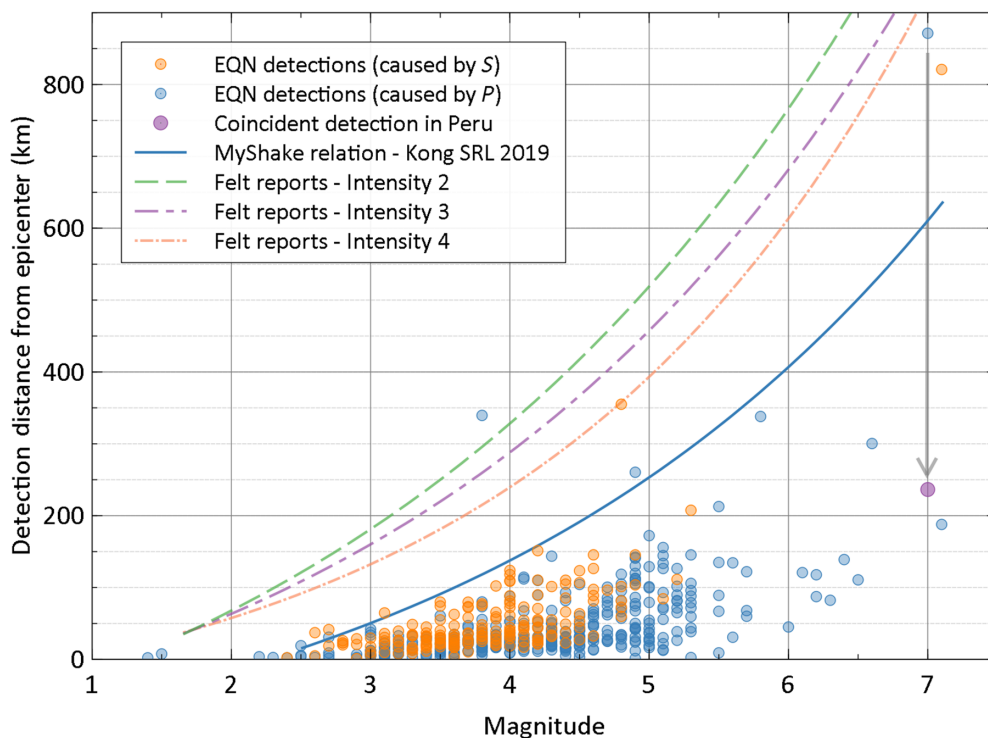
Figure 2. Distance between the location of the detection and the epicenter for 539 EQN associated detections as a function of magnitude. Blue and orange dots represent detections likely caused by *P* and *S* waves, respectively (although the causative seismic phase is uncertain for epicentral distances below about 50 km). One **M** 7 earthquake detected at more than 800 km epicentral distance was also detected in Peru at about 250 km epicentral distance (arrow and purple dot)—a rare example of a duplicate detection. For comparison, the blue curve approximates the maximum distance to which smartphones operating MyShake app can detect earthquakes (Kong *et al.*, 2019), whereas the three dashed lines approximate the 90% radial distance quantile of user-assigned intensities 2 (scarcely felt), 3 (weak), and 4 (largely observed) (based on the 1528 global earthquakes between 2011 and end of October 2020 with at least 100 felt reports collected by the European–Mediterranean Seismological Center (EMSC). The color version of this figure is available only in the electronic edition.

36 hr before the mainshock. The foreshock was not detected due to a lack of EQN users in California at the time. However, this foreshock led to EQN installations in sufficient number in the Los Angeles (LA) area (but not in the epicentral region) so that the mainshock was detected in LA, 200 km to the south of its epicenter. Seismic-wave propagation times from epicenter to LA, where it was detected, explains the unusually large detection latency of 40 s (see Table 2). In turn, the mainshock led to new EQN installations at shorter epicentral distances, leading to a drop of EQN detection latency to 8 s (median times) for the 27 subsequent detected **M** 2.7–4.6 aftershocks (see Table 2).

To evaluate EQN's intrinsic latency, the wave propagation time from the epicenter to the EQN's detection location is subtracted from alert issuance latency, using the most probable causative seismic phase. This not only gives an estimation of cumulative processing and transmission delays but is also an overestimate, as it implicitly assumes that acceleration (i.e., the monitored parameter) is large at seismic phase onset, when, in fact, it usually occurs later. Therefore, the minimum and median latencies (0.5 s and 4.3 s, respectively, Table 1) characterize the best detection latencies that the EQN system can offer; such fast detection is an achievement considering EQN's low-investment cost.

In summary, in regions with a significant app audience, EQN detection latency with respect to origin times for crustal earthquakes is comparable (5–8 s) to latencies observed in systems such as ShakeAlert (Table 2), and, in the best-case scenario, it could be as low as a couple of seconds.

EQN warning times
Warning time is defined for a given target intensity as the time delay between the publication of the alert and the *S* wave arriving at the locations of the users who experience that target intensity. Hence, the larger the warning time, the more time

explains why the median detection time was around 7–8 s in Italy and United States, where all detected earthquakes were onshore and at crustal depth (<40 km) compared to 17 s in Chile, where a significant proportion of detected earthquakes were offshore and/or at intermediate depth (Table 1).

A limited comparison of earthquake detection times can be performed with ShakeAlert—the operational EEW system that aims to cover the West Coast of the United States with 1700 seismic stations (Given *et al.*, 2018; Kohler *et al.*, 2018). Four earthquakes—the **M** 7.1 Ridgecrest mainshock and three of its aftershocks ranging in magnitude from 3.8 to 4.5—were detected by both the systems. Excluding the case of the mainshock (discussed subsequently), EQN latencies are larger by an average 1.6 s (7.6 s vs. 6.0 s averages for EQN and ShakeAlert, respectively), which is rather small considering the difference in technology levels. The Ridgecrest sequence exemplifies how EQN performance can rapidly change due to sudden app adoption. This sequence started with an **M** 6.4 foreshock

TABLE 1
Summary Statistics of Earthquake Detections

Country	Chile	United States	Italy	Total
Detections	458	70	22	550
Detections associated with known earthquakes	449	70	20	539
Available accelerometric records	328	69	13	410
Magnitude (min, max)	1.4, 7.1	2.2, 7.1	2.4, 5.1	1.4, 7.1
System detection delay with respect to origin time (min, median, max in seconds)	4.8, 17.2, 209.0	4.3, 8.1, 42.5	3.4, 7.3, 11.0	3.4, 15.4, 209.0
System detection delay with respect to passing of triggering seismic wave (min, median, max in seconds)	0.5, 4.3, 12.1	2.0, 4.6, 10.2	1.8, 4.5, 5.9	0.5, 4.3, 12.1
False detection rate (%)	2.0	0.0	9.1	2.0
Nighttime/daytime ratio	2.7	11.3	8.0	3.1
Source of catalog	CSN	USGS	INGV	

Associated detections are the number of Earthquake Network (EQN) detections for which it was possible to identify the causative earthquake. The accelerometric record column gives the number of detections for which accelerometric data are available within 20 km of the detection location. Detection delays of the EQN system were computed with respect to the earthquake origin time and the theoretical arrival time of the most likely causative seismic phase. False detection rate is the ratio between the number of false detections and the total number of detections, whereas the nighttime/daytime ratio is computed considering that day (7:00 a.m. to 10:59 p.m.) lasts twice the night. CSN, Centro Sismologico Nacional, Chile; INGV, Istituto Nazionale Geologia e Vulcanologia, Italy; USGS, U.S. Geological Survey.

TABLE 2
Detection Latencies for the Four Earthquakes Detected by Both ShakeAlert and EQN

Magnitude	Origin Time (yyyy/mm/dd hh:mm:ss.ss)	ShakeAlert Detection Delay (s)	EQN Detection Delay (s)	EQN Detection Distance (km)
7.1	2019/07/06 03:19:53.04	6.9	40.0	188
4.5	2019/10/15 05:33:42.81	5.6	7.2	3
3.8	2019/12/05 08:55:31.65	5.7	5.4	10
3.9	2019/12/12 08:24:32.60	6.8	10.4	20

These four earthquakes were detected in California, and they followed the **M** 7.1 Ridgecrest mainshock. ShakeAlert detection times were retrieved from Chung *et al.* (2020) for the **M** 7.1 Ridgecrest earthquake in California and from earthquake hazards program (see Data and Resources) for the others.

the user has to prepare for the incoming shaking. It is computed for the slower and stronger S wave, and assumes that the P wave is imperceptible, and that, from a user point of view, this is the delay between the alert issuance and the perceived tremor. It also assumes that the maximum intensity begins with the onset of S wave. Warning times have been computed for target intensities 4 (largely observed), 5 (strong), or 6 (slightly damaging) for all detected earthquakes worldwide greater than **M** 4.5 in Italy and United States and greater than **M** 5 in the rest of the world. Intensities with respect to radial distance were estimated using intensity predictive equations (IPEs) according to the validity domain of the considered IPE. Region-specific IPE were used in the western United States (Atkinson *et al.*, 2014) and Italy (Tosi *et al.*, 2015) for crustal earthquakes (focal depth between 0 and 40 km). For all

other regions, including deeper earthquakes, the same IPE (Allen *et al.*, 2012) was used. Because this earthquake dataset is global, for the sake of homogeneity, earthquake parameters were all taken from the U.S. Geological Survey (USGS).

According to these estimations, within the 72 detected earthquakes greater than **M** 4.5 or 5, EQN issued early warnings for target intensity 4 for 53 (74%) earthquakes (i.e., on average twice a month) that were located in 11 countries in North, Central and South America, Europe, and Asia (Figs. 3 and 4). Among these, 18 events also benefited from a warning for target intensity 5, and for two earthquakes there was a warning for target intensity 6: 26 July 2019 **M** 6.2 Panama and 26 November 2019 **M** 6.4 Albania. As expected, for a given target intensity, warning times increased with increasing magnitude, and, for a given earthquake, they
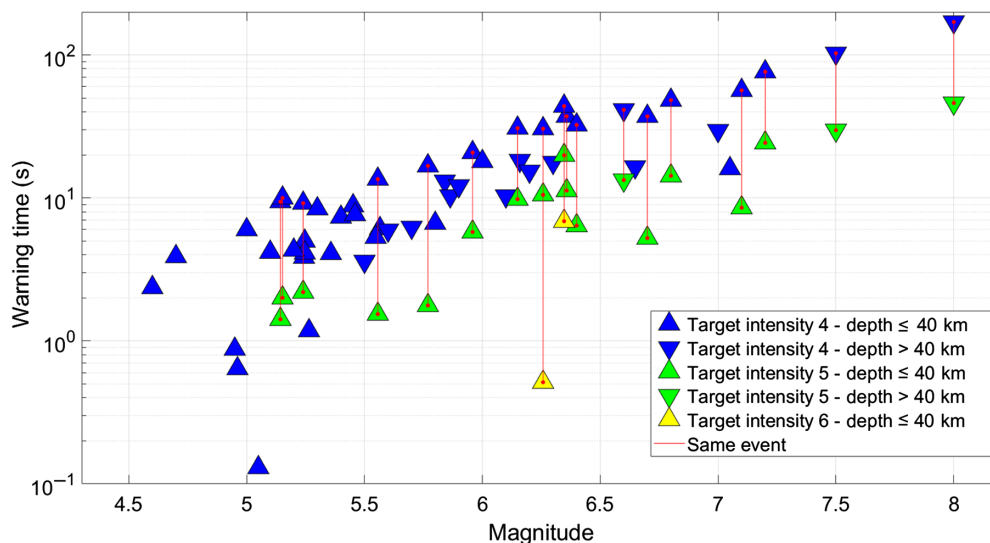
Figure 3. Estimated warning times for the 53 earthquakes detected worldwide with magnitude equal or greater than 4.5 with positive warning time. Blue, green, and yellow triangles depict warning times for target intensities 4, 5, and 6, respectively. Crustal and deep earthquakes are shown by triangles and inverted triangles, respectively. Warning times related to the same event are connected by red lines. For sake of clarity, magnitude is altered by a random shift of ±(0.03, 0.06) for earthquakes sharing the same magnitude. The color version of this figure is available only in the electronic edition.

decreased with increasing target intensities. For earthquakes greater than **M** 6, estimated warning times were typically more than 10 s for target intensity 4 and more than 5 s for target intensity 5 (see Fig. 3), long enough for the user to take protective measures.

The warning time for target intensity 6 for the Panama earthquake was too short for individual protective action. However, for the Albania earthquake, which struck at night and killed 51 people, a warning time of 6.9 s for intensity 6 has been estimated through the IPE, for a detection delay of 5.1 s after its occurrence and the location of the detection 20 km from its epicenter. According to the IPE, the isoseismal for intensity 6 was 34 km from the epicenter compared to 45 km from the empirical intensity–distance curve derived from about 4000 eyewitnesses' reports crowdsourced for this event (Bossu *et al.*, 2020). This implies that the warning times derived from the IPE is likely underestimated by about 2 s for intensity 6, leading to a warning time for "slightly damaging" shaking exceeding 8 s. Based on the spatial distribution of EQN users at the time of the earthquake, assuming 100% delivery success, and neglecting the transmission delay of the alert, we estimate that 1005 of them received the early warning for intensity 6, 231 for intensity 5, and 632 for intensity 4. With approximately 800,000 inhabitants within 40 km of the epicenter, the proportion of warned individuals remains small in this case. Still, it proves that EQN can offer significant warning time for damaging shaking levels and so has the potential to lower individual seismic risk for its users.
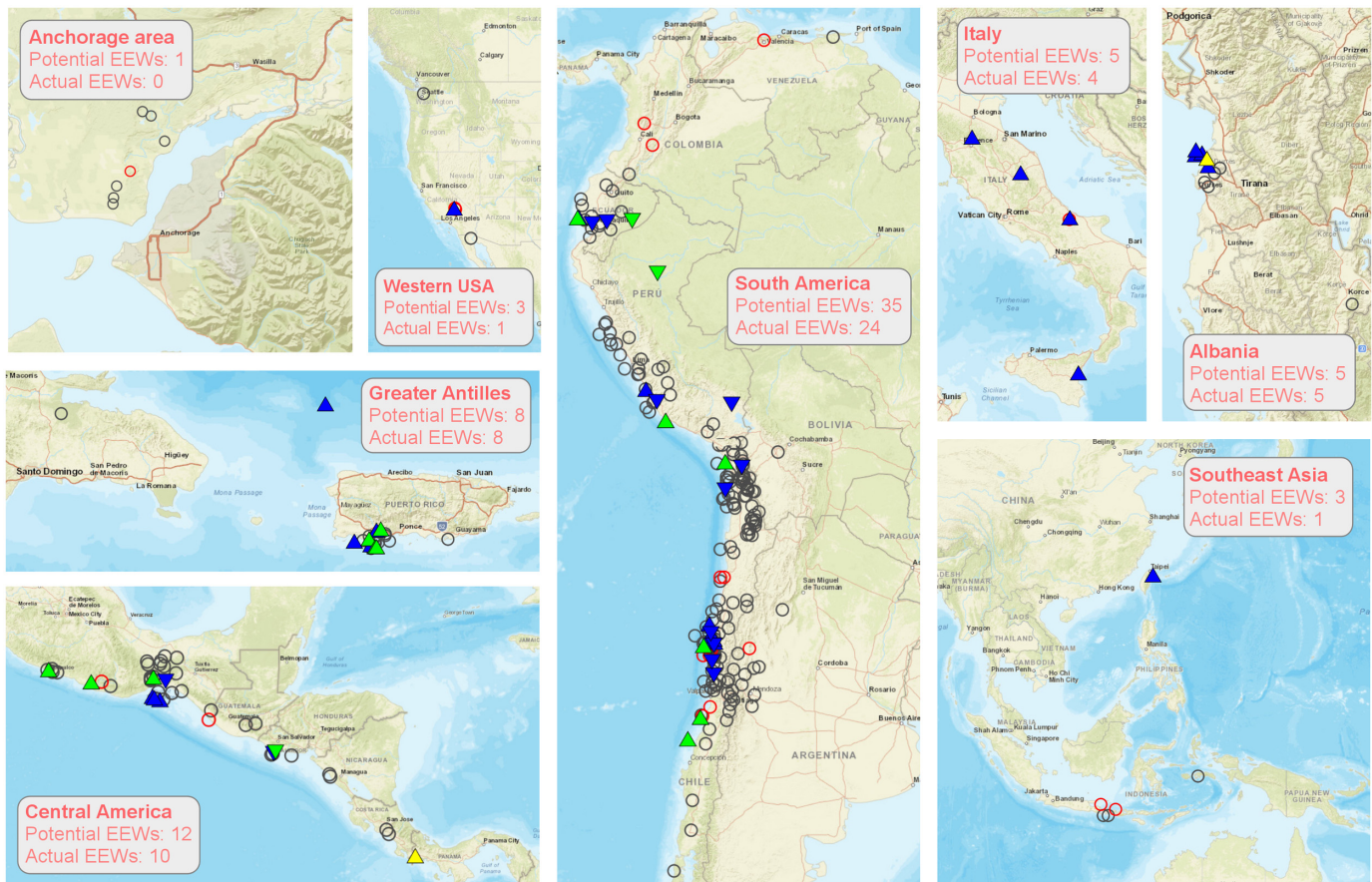
Do EQN users take protective actions after a warning?

The reaction to, and understanding of, early warning has been assessed by an online survey of EQN users in the felt area of the 26 May 2019 **M** 8 Peru earthquake to evaluate EQN's efficiency at individual risk reduction. This earthquake had a focal depth of 120 km and generated two EQN detections —one in Peru and one in Ecuador. Alerts were issued for 599 users for intensity 5 and 54,228 for intensity 4, respectively.

There were 61,863 users within 1500 km of the epicenter, a distance in which USGS and European–Mediterranean Seismological Center estimate that the intensity felt was between 3 and 4. About 2625 self-selected over 18 yr old participants responded to the questionnaire; over ⅔ of them declared to be between 500 and 1000 km from the epicenter at the time of the earthquake—a range containing the capital cities of Quito and Lima. Most respondents (82%) declared previous earthquake experiences, and 25% answered that they had experienced an EQN EEW before. About 72% were convinced or strongly convinced of the usefulness of the app, which confirms previous studies about public expectations for EEWs (e.g., Becker *et al.*, 2021). Among these 2625 self-selected respondents, 1663 had the app at the time of the earthquake, whereas the others installed it following the earthquake. Those who already had the app described various experiences: 34% received EQN notification before feeling the shaking as expected from a PEEW system, 35% received it after having felt the shaking, 11% received the notification but did not feel the earthquake, 14% did not receive the notification while feeling the shaking, and 6% neither received the notification nor felt the earthquake.

Importantly, among the users who received the notification before feeling the shaking, 79% understood that a tremor was about to hit. This means that they had a good comprehension of what an early warning is; but, when asked about their reaction (Table 3), only 25% performed "drop, cover, and hold." A major concern was to warn relatives nearby (55%) or for the ones not in immediate proximity through social media (22%). In addition, 35% waited for the shaking. These results are consistent with findings from Nakayachi

Figure 4. Geographical distribution of the 53 earthquakes for which a positive warning time is determined, shown as triangles (see Fig. 3 for legend). All other EQN-detected earthquakes of magnitude **M** 4.5 or above are represented by circles (in red) when the maximum onshore intensity reached or exceeded intensity 4 (for which an EEW is theoretically possible) and in gray otherwise. The number of EEW in the legends indicates the number of positive warning times at intensity 4. The color version of this figure is available only in the electronic edition.

et al. (2019), who showed that following an EEW in Japan, people mentally prepared rather than took actual safety actions.

This single study based on self-selected participants and on a single case confirms that a low-cost smartphone based PEEW system can offer an actual early warning to some users even if the alert dissemination delay is unknown and may differ from one user to the next. Despite the lack of information about the magnitude and some users experiencing what they perceived as false alerts (namely alerts for real earthquakes that, however, are not felt at the user location), levels of satisfaction and trust are still high. In fact, the survey showed that 82% of users would appreciate being informed about an incoming earthquake, even if it did not reach damaging levels of intensity. However, in its current setting, and although the meaning of the notification is often understood, it only leads to adequate protective actions in a minority of cases, possibly because it does not answer an expressed priority need, which is to inform loved ones who may not have the app. The fact that EQN is appreciated by most of its users suggests that, despite EQN's inability to systematically guarantee an early warning or estimate an event's magnitude, such a service combining early warning and rapid detection of felt earthquakes is valued by its users and constitutes a progress in public earthquake information.

Discussion

The EQN initiative exploits smartphone ubiquity to create an operational network that provides an early warning service to its users. This service differs from conventional services as EQN's alerting strategy is not based on predicted intensity, which in some ways simplifies the service behavior. Indeed, even when earthquake source parameters (magnitude and location) are accurately determined, ground-motion variability means that a conventional service sometimes has users receive an undue alert, because the predicted intensity is overestimated or, more commonly, has users not receive the expected alert because of underestimation of the intensity (Minson *et al.*, 2019). Instead, EQN provides both PEEW and rapid information (preliminary epicenter and time of the event) for small-magnitude felt earthquakes for which no early warning is

TABLE 3

Summary of Responses to Question 16 in the Online Survey of EQN Users that was Carried Out in Peru Following the 26 May 2019 M 8 Peruvian Earthquake

Q16. What did you do when you received the notification?	Percentage
I warned my relatives physically present with me.	54.6%
I waited for the first vibrations of the earthquake.	35.4%
I went to a safe place in my house (under a table, etc.) dropped, covered, and hold on.	25.0%
I warned my relatives through social media, SMS, and so forth.	22.1%
I ran outside.	9.6%
Nothing	2.8%
Other	2.8%

Participants were allowed to give multiple answers. Base: Users who received the notification and felt the earthquake afterward (n = 571). Several answers possible.

possible, which, as shown by user survey, is valued by users. It is noteworthy that following the Ridgecrest earthquake, ShakeAlert users' complaints of not having received an alert for felt shaking led to a lowering of the target intensity to 3. Considering aforementioned limitations, this leads to an actual ShakeAlert service not far from the one offered by EQN (Cochran and Husker, 2019). In Mexico, extending early warning services to also offer rapid public information for felt earthquakes seems to be an appreciated feature, with an alert being considered as false only if an earthquake did not actually occur (Allen *et al.*, 2018). In addition, following feedback from Mexico's users, it was proposed that PEEW messages do not include intensity, because it is often confused with magnitude, and may create difficulties with interpretation and hamper decisions to take protective actions (Allen *et al.*, 2018). The EQN users' survey, which also took place in Latin America, presents further support for these findings, though EQN, like any app, is based on self-selective participation, and its users' feedback may not be a representative sample of the opinion of a global audience. As the evidence implies that the lack of intensity prediction is not a major impediment, it can be concluded that EQN's early warning and rapid information services are a significant improvement from existing rapid public information systems for seismically active regions of the globe not yet covered by conventional PEEWs.

Data and Resources

Datasets analyzed in this article are available through GeoForschungsZentrums (GFZ) Data Services at the following links. R. Steed, R. Bossu, F. Finazzi, I. Bondár, and L. Fallou (2021). Analysis of detections by the Earthquake Network app between 2017-12-15 and 2020-01-31. V. 0.9. GFZ Data Services, https://doi.org/10.5880/

fidgeo.2021.007. R. Steed, R. Bossu, F. Finazzi, I. Bondár, and L. Fallou (2021). Analysis of strong motion waveforms near the locations of detections by the Earthquake Network app in Chile, the USA, and Italy. V. 0.9. GFZ Data Services., https://doi.org/10.5880/fidgeo.2021.002. L. Fallou, R. Bossu, R. Steed, F. Finazzi, and I. Bondár. A questionnaire survey of the Earthquake Network app's users in Peru following an **M** 8 earthquake in 2019. V. 0.9. GFZ Data Services (2021). https://doi.org/10.5880/fidgeo.2021.001. Earthquake hazards program is available at http://earthquake.usgs.gov (last accessed July 2021).

Declaration of Competing Interests

The authors declare no competing interests.

Acknowledgments

References

Allen, R. M., and D. Melgar (2019). Earthquake early warning: Advances, scientific challenges, and societal needs, *Annu. Rev. Earth Planet. Sci.* **47,** 361–388.

Allen, R. M., E. S. Cochran, T. J. Huggins, S. Miles, and D. Otegui (2018). Lessons from Mexico's earthquake early warning system, *Eos Earth Space Sci. News* **99,** doi: 10.1029/2018EO105095.

Allen, T. I., D. J. Wald, and C. B. Worden (2012). Intensity attenuation for active crustal regions, *J. Seismol.* **16,** 409–433.

Ancheta, T. D., J. P. Stewart, and N. A. Abrahamson (2011). Engineering characterization of earthquake ground motion coherency and amplitude variability, *Effects of Surface Geology on Seismic Motion. 4th IASPEI/IAEEInternational Symposium*, University of California Santa Barbara, 1–12.

Atkinson, G. M., C. B. Worden, and D. J. Wald (2014). Intensity prediction equations for North America, *Bull. Seismol. Soc. Am.* **104,** 3084–3093.

Becker, J. S., S. H. Potter, L. J. Vinnell, K. Nakayachi, S. K. McBride, and D. M. Johnston (2020). Earthquake early warning in Aotearoa New Zealand: A survey of public perspectives to guide warning system development, *Humanit. Soc. Sci. Comm.* **7,** 1–12.

Becker, J. S., S. H. Potter, L. J. Vinnell, K. Nakayachi, S. K. McBride, and D. M. Johnston (2021). Earthquake early warning in Aotearoa New Zealand: A survey of public perspectives to guide warning system development, *Humanit. Soc. Sci. Comm.* **7,** 1–3.

Bossu, R., L. Fallou, M. Landès, F. Roussel, S. Julien-Laferrière, J. Roch, and R. Steed (2020). Rapid public information and situational awareness after the November 26, 2019, Albania earthquake:
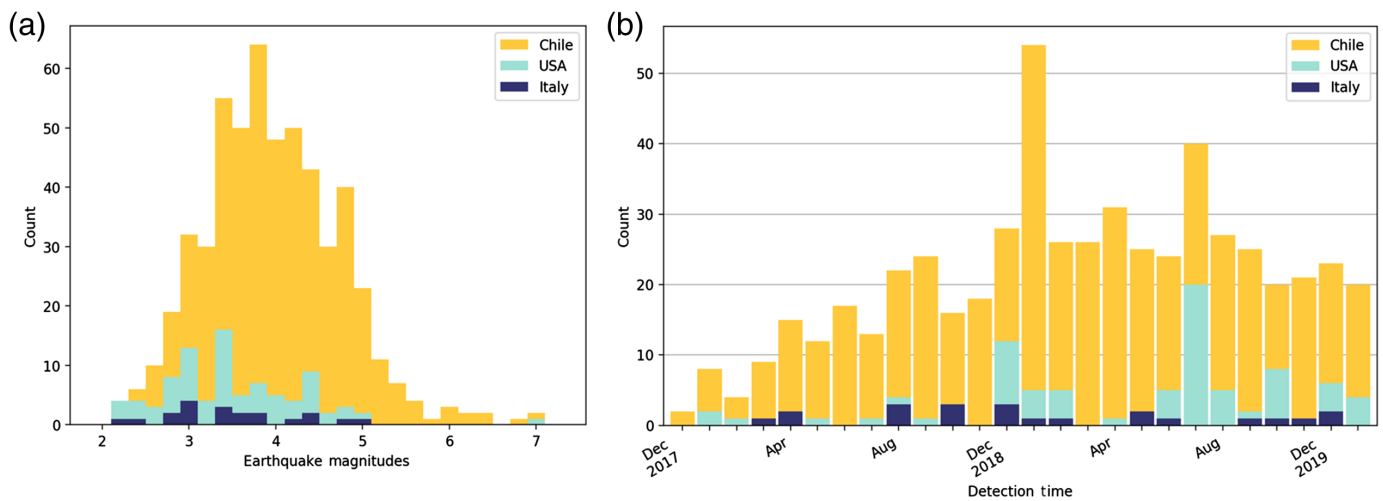
Lessons learned from the LastQuake system, *Front. Earth Sci.* **8,** 235, doi: 10.3389/feart.2020.00235.

Brooks, B. A., M. Protti, T. Ericksen, J. Bunn, F. Vega, E. S. Cochran, C. Duncan, J. Avery, S. E. Minson, E. Chaves, *et al.* (2021). Robust earthquake early warning at a fraction of the cost: ASTUTI Costa Rica, *AGU Adv.* **2,** e2021AV000407, doi: 10.1029/2021AV000407.

Chung, A. I., M. A. Meier, J. Andrews, M. Böse, B. W. Crowell, J. J. McGuire, and D. E. Smith (2020). ShakeAlert earthquake early warning system performance during the 2019 Ridgecrest earthquake sequence, *Bull. Seismol. Soc. Am.* **110,** 1904–1923.

Cochran, E. S., and A. L. Husker (2019). How low should we go when warning for earthquakes? *Science* **366,** 957–958.

Cremen, G., and C. Galasso (2020). Earthquake early warning: Recent advances and perspectives, *Earth Sci. Rev.* **205,** 103184, doi: 10.1016/j.earscirev.2020.103184.

Finazzi, F. (2016). The earthquake network project: Toward a crowd-sourced smartphone-based earthquake early warning system, *Bull. Seismol. Soc. Am.* **106,** 1088–1099.

Finazzi, F. (2020a). The earthquake network project: A platform for earthquake early warning, rapid impact assessment, and search and rescue, *Front. Earth Sci.* **8,** 243, doi: 10.3389/feart.2020.00243.

Finazzi, F. (2020b). Fulfilling the information need after an earthquake: Statistical modelling of citizen science seismic reports for predicting earthquake parameters in near realtime, *J. Roy. Stat. Soc. A* **183,** 857–882.

Finazzi, F., and A. Fassò (2017). A statistical approach to crowd-sourced smartphone-based earthquake early warning systems, *Stoch. Environ. Res. Risk Assess.* **31,** 1649–1658.

Given, D. D., R. M. Allen, A. S. Baltay, P. Bodin, E. S. Cochran, K. Creager, R. M. de Groot, L. S. Gee, E. Hauksson, T. H. Heaton, *et al.* (2018). *Revised technical implementation plan for the ShakeAlert system—An earthquake early warning system for the West Coast of the United States*, U.S. Geol. Surv. Open-File Rept. 2018-1155, doi: 10.3133/ofr20181155.

Hsiao, N. C., Y.-M. Wu, T.-C. Shin, L. Zhao, and T.-L. Teng (2009). Development of earthquake early warning system in Taiwan, *Geophys. Res. Lett.* **36,** L00B02, doi: 10.1029/2008GL036596.

Kohler, M. D., E. S. Cochran, D. Given, S. Guiwits, D. Neuhauser, I. Henson, R. Hartog, P. Bodin, V. Kress, S. Thompson, *et al.* (2018). Earthquake early warning ShakeAlert system: West coast wide production prototype, *Seismol. Res. Lett.* **89,** 99–107.

Kong, Q., R. M. Allen, L. Schreier, and Y. W. Kwon (2016). MyShake: A smartphone seismic network for earthquake early warning and beyond, *Sci. Adv.* **2,** e1501055 , doi: 10.1126/sciadv.1501055.

Kong, Q., R. Martin-Short, and R. M. Allen (2020a). Toward global earthquake early warning with the MyShake smartphone seismic network, part 1: Simulation platform and detection algorithm, *Seismol. Res. Lett.* **91,** 2206–2217.

Kong, Q., R. Martin-Short, and R. M. Allen (2020b). Toward global earthquake early warning with the MyShake smartphone seismic network, part 2: Understanding MyShake performance around the World, *Seismol. Res. Lett.* **91,** 2218–2233.

Kong, Q., S. Patel, A. Inbal, and R. M. Allen (2019). Assessing the sensitivity and accuracy of the MyShake smartphone seismic network to detect and characterize earthquakes, *Seismol. Res. Lett.* **90,** 1937–1949.

Lindell, M. K., and R. W. Perry (2021). The protective action decision model: Theoretical modifications and additional evidence, *Risk Anal.* **32,** 616–632.

Minson, S. E., A. S. Baltay, E. S. Cochran, T. C. Hanks, M. T. Page, S. K. McBride, K. R. Milner, and M.-A. Meier (2019). The limits of earthquake early warning accuracy and best alerting strategy, *Sci. Rep.* **9,** 1–13.

Minson, S. E., B. A. Brooks, C. L. Glennie, J. R. Murray, J. O. Langbein, S. E. Owen, T. H. Heaton, R. A. Iannucci, and D. L. Hauser (2015). Crowdsourced earthquake early warning, *Sci. Adv.* **1,** e1500036, doi: 10.1126/sciadv.1500036.

Nakayachi, K., J. S. Becker, S. H. Potter, and M. Dixon (2019). Residents' reactions to earthquake early warnings in Japan, *Risk Anal.* **39,** 1723–1740.

Suárez, G., D. Novelo, and F. E. Mansilla (2009). Performance evaluation of the seismic alert system (SAS) in Mexico City: A seismological and a social perspective, *Seismol. Res. Lett.* **80,** 707–716.

Tosi, P., P. Sbarra, V. De Rubeis, and C. Ferrari (2015). Macroseismic intensity assessment method for web questionnaires, *Seismol. Res. Lett.* **86,** 985–990.

Voosen, P. (2021). New Google effort uses cellphones to detect earthquakes, *Sci. News*, doi: 10.1126/science.abj2298.

Wood, M. M., D. S. Mileti, H. Bean, B. F. Liu, J. Sutton, and S. Madden (2018). Milling and public warnings, *Environ. Behav.* **50,** 535–566.

Xu, Y., J. P. Wang, Y. M. Wu, and H. Kuo-Chen (2017). Reliability assessment on earthquake early warning: A case study from Taiwan, *Soil Dynam. Earthq. Eng.* **92,** 397–407.

Appendix
Datasets used in analysis

Datasets were constructed from the events detected by the Earthquake Network (EQN) app between 15 December 2017 and 31 January 2020. This time range was chosen so that EQN's detection procedures would be stable during the entire period. There were 1792 detections during this period in 19 countries. To perform quantitative analysis, two subdatasets were extracted from this global dataset. These datasets are available as externally hosted supplemental material as Data S1 and Data S2 (see Steed *et al.*, 2021a in Data and Resources).

Data S1 is composed of 550 detections for examining the speed and location accuracy of EQN. Among the countries with a strong user base for the app, we chose to analyze the events in Chile, United States, and Italy due to the accuracy and completeness of their catalogs. Importantly, all three regions operate dense seismological station networks that are able to produce accurate event locations and magnitude estimates. An epicentral location inaccuracy of 15 km translates to a seismic phase arrival time change of 2–3 s, which can become important in the case of EQN due to its rapid response times. All three regions also have dense accelerometer networks whose records were used to validate the EQN triggers. The U.S. Geological Survey (USGS, U.S.A.) and Istituto Nazionale Geologia e Vulcanologia (INGV, Italy) catalogs of earthquake parameters were searched via International Federation of Digital Seismograph Networks (FDSN) requests,

Figure A1. (a) This stacked histogram shows that EQN detected earthquakes over a range of magnitudes in Chile, United States, and Italy. About 539 out of the 550 EQN detections studied were associated with earthquakes with published parameters. (b) A stacked histogram of the number of EQN detections per month in Chile, United States, and Italy. A growth in the number of detections can be seen for Chile and the United States over this period. The color version of this figure is available only in the electronic edition.

whereas the Centro Sismologico Nacional (CSN, Chile) catalog was provided upon request. Calculations of the P and S seismic phases used the ak135 model and were carried out by the ObsPy Python library (see following sections for other calculation of other fields). The distributions of Data S1 with respect to magnitude and detection date are depicted in Figure A1.

Data S2 was used for an analysis of EQN's early warning performance and consists of moderate-to-large magnitude earthquakes from around the world that were detected by EQN. This analysis employed intensity predictive equations (IPEs) to estimate the intensities felt in regions that were warned of imminent shaking by the EQN app. The IPE equations' validities limited the analysis to earthquakes $\mathbf{M} \geq 5$ in most of the world, and $\mathbf{M} \geq 4.5$ in Italy and United States (the equations are in the Calculation of Shaking Intensities section). The dataset is composed of 168 earthquakes and has 68 detections in common with Data S1. The main results from analysis of Data S2 can be seen in Figures 3 and 4. All of the earthquake parameters were obtained from the USGS catalog for consistency.

There were also three earthquakes that were detected twice by EQN; normally such duplicate detections are suppressed automatically, but all the three earthquakes were large-magnitude events ($\mathbf{M}$ 7.0, 7.5, and 8.0) that led to EQN making detections at distances far from the epicenters. These three duplicate detections have been removed from the dataset for clarity.

Association of detections with earthquakes

For the purposes of the analysis, it is important to associate each EQN detection with earthquakes parameters held in an institute's catalogs of events. The following procedure was used for association:

1. Earthquakes were selected from the catalog from 250 s before the time of the detection until 4 s afterward.
2. Earthquakes were selected that are also within the association distance defined by each earthquake's magnitude (see Fig. A2).

3. For each earthquake, the arrival time of the P waves at the EQN detection location was estimated using the ak135 model's speed of 8.04 km/s. The events whose P waves arrive within 90 s before the EQN detection and 10 s after the detection were chosen.
4. If multiple earthquakes remained in the selection, then the earthquake of the largest magnitude was chosen as the associated earthquake.

Causal seismic phase of EQN detections

It has been found that EQN detections can be triggered by either P or S seismic phases (see Fig. A3). The EQN detections were split heuristically into being caused by P or S phases using the criteria:

Caused by S if : (detection delay w.r.t. $S > 0$ s)

$$\& \ (\text{detection delay w.r.t. } P > 6 \text{ s}). \tag{A1}$$

Distinguishing between P and S phases is less clear within 50 km of the epicenter, because both arrive within a short interval of time. In addition, the EQN detections are triggered by strong motion due to the relative insensitivity of the smartphone accelerometers, and the P/S phase arrival does not exactly coincide with the onset of motion strong enough to cause a detection.

Calculation of shaking intensities

IPEs were used to create the columns in the datasets (Data S1 and S2) and for the analysis of early warning times presented in the article. An IPE predicts the total felt intensity of shaking with respect to hypocentral distance for a given magnitude of earthquake. For a given delay from the origin time of an earthquake, the distance of the S phase from the epicenter can be calculated using the ak135 model, and the intensity of shaking for this distance can then be calculated using the IPE. Alternatively, the distance at which the intensity reaches a certain value can be found, and then the time at which the S phase passes this distance can be calculated to estimate whether there would be time for a warning to be given to people at this intensity.

To convert between epicentral and hypocentral distance, the following equation was adopted:

$$r^2 = d^2 + 4R(R - d)\sin^2\left(\frac{s}{2R}\right), \tag{A2}$$

in which r is the hypocentral distance, d is the hypocentral depth, R is the Earth's radius, and s is the epicentral distance.

For most earthquakes, the IPE from Allen $et\ al.$ (2012) were used; this formula is only valid for magnitudes $\mathbf{M} > 5$, and so we restricted the analysis accordingly:

$$\text{Intensity}$$
$$= \begin{cases} 2.085 + 1.428M + 1.402\ln\sqrt{r^2 + R_m^2}, & r < 50\,\text{km} \\ 2.085 + 1.428M + 1.402\ln\sqrt{r^2 + R_m^2} + 0.078\ln\frac{r}{50}, & r \geq 50\,\text{km} \end{cases}, \tag{A3}$$

in which M is the earthquake magnitude and:

$$R_m = -0.209 + 2.042\exp(M - 5). \tag{A4}$$

For the Italian earthquakes, the IPE from Tosi $et\ al.$ (2015) was employed for crustal earthquakes (focal depth between 0 and 40 km):

$$\text{Intensity} = -2.15\log_{10}r + 1.03M + 2.31. \tag{A5}$$

For the western United States, the IPE from Atkinson $et\ al.$ (2014) was used:

$$\text{Intensity} = 0.309 + 1.864M - 1.672\log_{10}\sqrt{r^2 + 14^2}$$
$$- 0.00219\sqrt{r^2 + 14^2} + 1.77\max\left(0, \log_{10}\frac{r}{50}\right)$$
$$- 0.383M\log_{10}\sqrt{r^2 + 14^2}. \tag{A6}$$

Comparisons with strong-motion waveforms

For Data S1 (detections in Chile, United States, and Italy), a search was made using the FDSN protocol for accelerometer
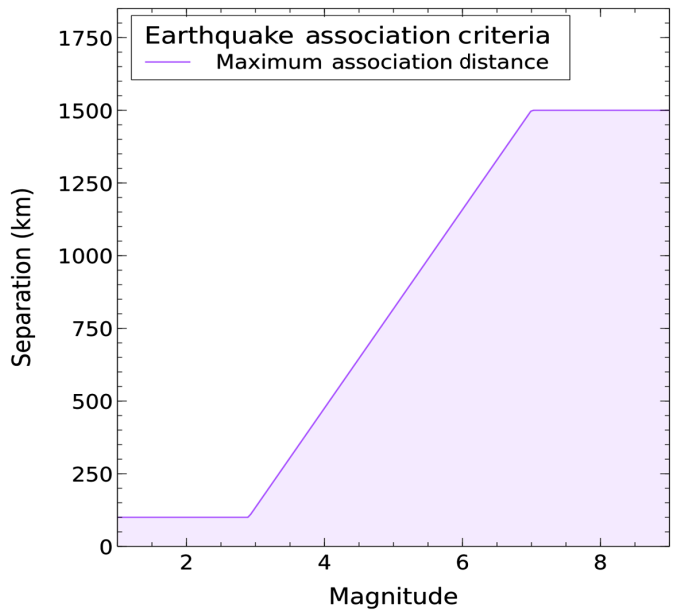

Figure A2. Association between an earthquake and EQN detection is allowed only if the separation between the epicenter and the EQN detection location is less than a threshold distance dependent upon the earthquake's magnitude, as shown previously. The color version of this figure is available only in the electronic edition.

station waveforms within 20 km of each EQN detection. The waveforms were detrended, calibrated as acceleration measurements, and band-pass filtered between 0.5 and 12 Hz. The waveform was also shifted in time to account for the difference in radial distance for the EQN detection location and the strong-motion station with respect to the epicenter of the earthquake. The shift crudely assumed a P-wave velocity of 8 km/s, and the time shift was less than 1 s in the majority of cases. The correction ensured that there was no confusion in causality for the analysis, whereby the EQN detection occurred before the strong motion arrived.

Accelerometric data were found for 410 of the 550 detections in Data S1. The analysis demonstrated a strong correlation between strong motion and the EQN detections, as would be expected, and that it was also found that even small accelerations were able to cause EQN triggers (see Fig. A4). The analysis also corroborated that the detections can be triggered by both P and S seismic phases (see also Fig. A3, which shows this through a timing analysis), although it should be remembered that the strong motion necessary to cause triggers might follow a few seconds after the passing wavefront.

Survey of Peruvian EQN users following the M 8 earthquake in Peru on 26 May 2019

The survey was carried out from 23 July to 19 August 2019. It was initiated through a message sent for technical reasons to all Spanish language users of the EQN app, linking to an online
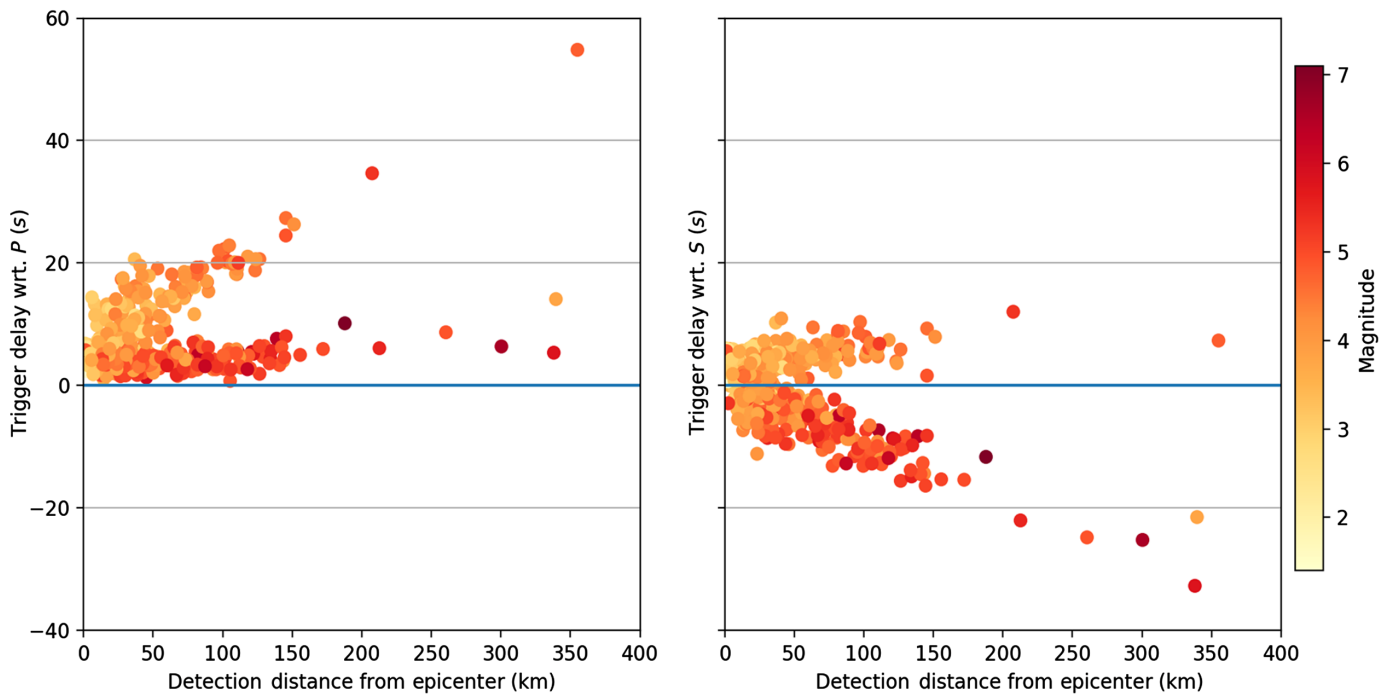
Figure A3. Determination of whether EQN detections follow the *P* or *S* seismic phase using Data S1. The arrival of the *P* and *S* phases at the detection location was calculated using the ak135 model, and the latency between each phase arrival and the detection time is plotted against separation between the detection location and the epicenter. It can be seen that detections closely follow the passing of either the *P* or *S* phases, and that EQN tends to detect larger magnitude earthquakes using the *P* wave. The color version of this figure is available only in the electronic edition.
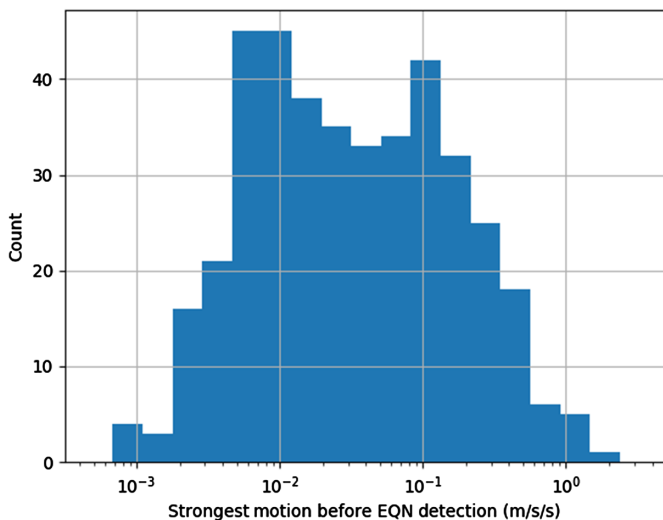

Figure A4. Histogram of the strongest acceleration found in the closest strong-motion recording for each EQN detection in the 30 s period before detection. The results are only approximate, because the level of shaking can significantly vary even over a distance of 10–20 km (Ancheta *et al.*, 2011). The color version of this figure is available only in the electronic edition.

questionnaire in Spanish (using google forms). The questionnaire was designed based on the existing literature (Wood *et al.*, 2018; Nakayachi *et al.*, 2019; Lindell and Perry, 2021) and two preliminary interviews with Peruvian EQN users. The questions aimed to assess expectations for earthquake early warning (EEW), understanding of the EQN warnings, and reactions to the warnings and to false or late alerts. It included both open-ended questions and Likert scales, and took about 8 min to complete. In compliance with the European General Data Protection Regulation, no private data were collected, and explicit consent was obtained for data collection from participants. The original version and an English translation of the questionnaire can be found in Fallou *et al.* (2021; see Data and Resources) along with the results of the survey. In addition, this survey will be discussed in more depth in a separate article.